

TTT and TTP Diagrams of Quenching Sensitivity of Al-9.0Zn-2.5Mg-1.5Cu-0.15Zr-0.2Sc Alloy

Dai Xiaoyuan, Xiong Chaoyu, Li Ni, Luo Yibing

Key Laboratory of Lightweight of Engineering Vehicle and Reliability Technology, Changsha University of Science and Technology, Changsha 410114, China

Abstract: The time-temperature-transformation (TTT) curve and time-temperature-property (TTP) curve of Al-9.0Zn-2.5Mg-1.5Cu-0.15Zr-0.2Sc alloy were determined by an interrupted quenching technique. Phase transformations were investigated by transmission electron microscope (TEM), differential scanning calorimetry (DSC) and X-ray diffraction (XRD). The result shows that when the holding time is prolonged at a certain temperature, the electro-conductivity of the specimens tends to increase and the hardness will decrease. Microstructure observation indicates that as the time increases, a lot of large equilibrium rod-shaped η (MgZn₂) phases precipitate in the matrix and grow rapidly, which results in the loss of solutes during the quenching process and weakens the subsequent aging strengthening effect. The main reasons for the precipitation of η particles are the rapid diffusion of solute atoms and the strong driving force for phase transformation. Quenching sensitive temperature range is 270~390 °C. Consequently, in the quenching sensitive temperature range, it is necessary to increase the cooling rate properly to obtain high mechanical properties. And in other temperature ranges, the cooling rate should be appropriately lowered to control the residual stress.

Key words: Al-9.0Zn-2.5Mg-1.5Cu-0.15Zr-0.2Sc alloy; TTT curve; TTP curve; precipitate free zone

Al-Zn-Mg-Cu alloys are widely used in the aviation field owing to their high strength, low density, and excellent formability^[1,2]. In order to acquire excellent mechanical performance, quenching is a crucial process because insufficient quenching will lead to uneven structure properties along the section and reduce alloy performance after ageing^[3-6]. This phenomenon is known as quenching sensitivity, and many researchers have done a lot of works about it^[7-10].

Furthermore, adding rare-earth elements into aluminum alloy is an effective way to enhance the performance of aluminum alloy^[11-14]. Scandium (Sc) can refine the grain and increase alloy strength and thermal stability. Abundant Al₃Sc particles will be divided into two different forms^[15]. The primary Al₃Sc formed in solidification can refine the grain^[16,17], and the secondary Al₃Sc formed during the subsequent process can inhibit recrystallization and obtain significant precipitation hardening^[18]. Nevertheless, the cost of Sc is too high. It is expected to find a lower priced ra-

re-earth element which can replace Sc. Researchers found that Zirconium (Zr) is a suitable element. Not only can Zr replace some part functions of Sc, but also the price is lower. When Sc and Zr are added together, the Al₃(Sc, Zr) particles can inhibit recrystallization effectively and achieve an enhancement effect^[19-21].

Currently, there are many ways to assess the quenching sensitivity of aluminum alloys, for example, end quenching test, TTP (time-temperature-properties) curves, TTT (time-temperature-transformation) curves and CCT (continuous-cooling-transformation) curves^[9,10,22-24]. However, there are few studies on the quenching sensitivity of aluminum alloy with Sc and Zr elements. In this work, the quenching sensitivity of Al-Zn-Mg-Cu-Zr-Sc alloy was determined by the TTT and TTP curves.

1 Experiment

Received date: March 14, 2018

Foundation item: Key Laboratory of Lightweight and Reliability Technology for Engineering Vehicle, Education Department of Hunan Province (2016kfjj06)

Corresponding author: Dai Xiaoyuan, Ph. D., Associate Professor, College of Automotive and Mechanical Engineering, Changsha University of Science and Technology, Changsha 410114, P. R. China, E-mail: 542047849@qq.com

Copyright © 2019, Northwest Institute for Nonferrous Metal Research. Published by Science Press. All rights reserved.

The sheets of the experimental alloy were orderly produced through homogenization, extrusion, hot rolling, intermediate annealing, and cold rolling. The actual chemical composition is Al-8.95Zn-2.43Mg-1.45Cu-0.15Zr-0.21Sc (wt%). The dimension of the aluminum alloy used in the experiment is 16 mm×16 mm×3 mm. After solution heat treated at 455 °C for 2 h, the specimens were quickly transferred into the salt bath furnace at different temperatures (240, 270, 300, 330, 360, 390, 420 °C). The transfer time is less than 3 s. After isothermal holding for the corresponding time (5, 20, 100, 600, 1500 s), the specimens were water quenched at room temperature and then artificially aged at 120 °C for 24 h.

The hardness of the samples was measured by HV-1000 type Vickers hardness tester under the load of 10 kg. Each sample was measured at least three times and the results were averaged. The electrical conductivity of the specimens was tested by D60K metal testing device. NETZSCH STA449C was used for DSC detection at the heating rate of 10 °C/min. XRD experiments were carried out on a rotating anode with a Cu target using a D/Max2500. The micro-structure was further studied by TEM, TECNAIG_20, with 200 kV accelerating voltage. TEM samples were prepared by mechanical grinding to a thickness of 80 μm and pressed to a disc with 3 mm in diameter, and then electro-polished using a twin-jet polishing machine with 30% HNO₃ and 70% CH₃OH solution at -25 °C, and the applied voltage is 15~20 V.

2 Results and Discussion

2.1 Electro-conductivity measurement and TTT curve

Fig.1 indicates the relationship between isothermal treatment and electro-conductivity of quenched samples. As shown in the picture, within a certain temperature range, prolonging the holding time will increase the electro-conductivity of alloy. The electro-conductivity increased rapidly at the beginning and then kept steady. We can see that in Fig.1a, at the relatively low temperatures, such as 240~300 °C, the increment rate of electro-conductivity gradually increases as temperature rises. At 300 °C for 100 s, the electrical conductivity of the material increases by about 60%. In contrast, the conductivity rises by less than 20% at 240 °C. We can see in Fig.1b that at the relatively high temperatures ranging from 330 °C to 390 °C, the electro-conductivity decreases with increasing the temperature. The conductivity rises fastest at 330 °C, which reaches to 71% after 100 s.

When the alloy was directly water quenched to room-temperature after solution heat treatment, the electro-conductivity is 24.83% IACS, which implies a supersaturate solid solution state. If the samples were treated at 455 °C for 2 h, isothermally held at 330 °C for 26 h, and

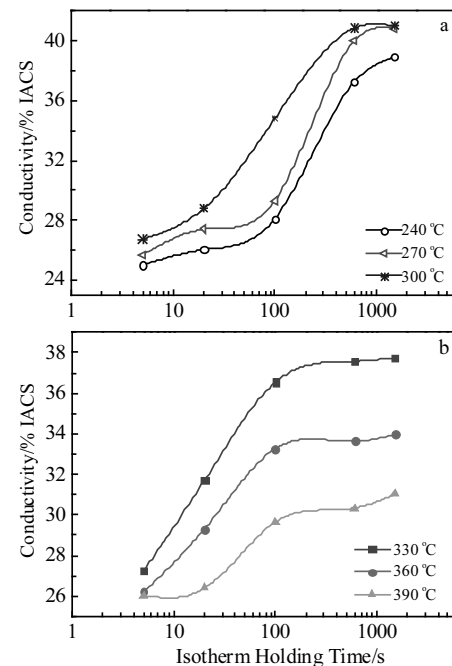


Fig.1 Effect of isothermal treatment on conductivity of as-quenched samples: (a) 240~300 °C and (b) 330~390 °C

then water-quenched to room temperature, the electro-conductivity is 41.38% IACS, which represents a complete decomposition of the supersaturate solid solution. Fig.2 shows the TTT curves of the samples obtained by a solution isothermal holding electro-conductivity measurement method. The shape of the TTT curves is usually similar to the English letter "C" and the nose temperature is 330 °C. The time for experimental alloy to complete 10% of its maximum transformation at 330 °C was only about 4 s. Clearly, the quenching sensitivity of specimens is high.

2.2 Hardness measurement and TTP curve

Fig.3 shows the hardness profiles of experimental alloys after different isothermal treatments followed by aging. It is obvious that with prolonging the holding time, the sample hardness gradually decreases. Furthermore, the difference in holding temperature will lead to the difference of hardness decreasing rate. In the temperature range of 240~300 °C, hardness decreased faster at higher temperatures, as shown in Fig.3a. At 240 °C for 100 s, the hardness of the material decreased by only about 17%, while at 300 °C for 100 s, the hardness decreased by about 49%. However, in the relatively high temperature range of 330~420 °C, the hardness decreased slowly. At about 330 °C, hardness of the material decreased by about 55% after 100 s, while it only decreased by nearly 10% at 420 °C.

After the samples were thermally treated at 455 °C for 2 h, then water quenched and artificially aged at 120 °C

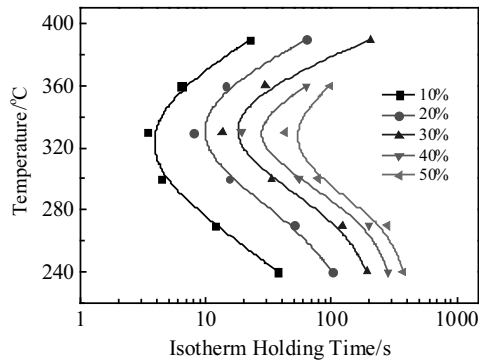


Fig.2 TTT curves of Al-9.0Zn-2.5Mg-1.5Cu-0.15Zr-0.2Sc alloy

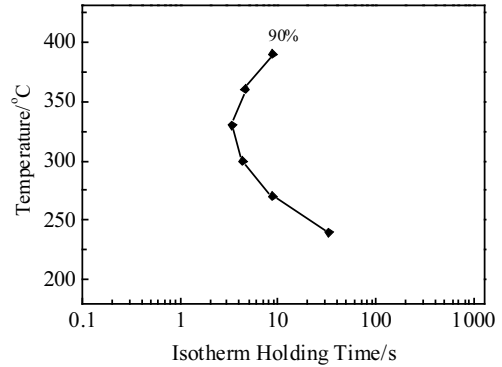


Fig.4 TTP curve of Al-9.0Zn-2.5Mg-1.5Cu-0.15Zr-0.2Sc alloy

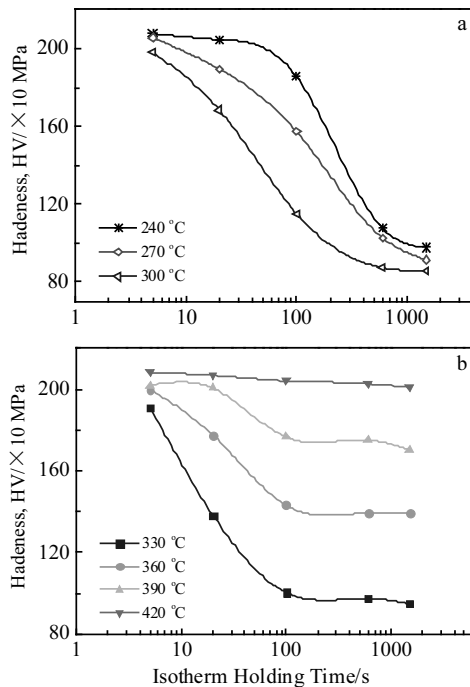


Fig.3 Effect of isothermal treatment on hardness of as-aged samples: (a) 240~300 °C and (b) 330~420 °C

for 24 h, the measured hardness HV is 2240 MPa, which is defined as the maximum property. According to the hardness data, we found the holding time and temperature corresponding to 90% of the maximum hardness, and then plotted the TTP curve (Fig.4). TTP curve can also describe the quenching sensitivity of aluminum alloy.

As shown in Fig.4, the TTP curve of the alloy also has a nose temperature. It is about 330 °C. When the hardness of the alloy fell by about 10% at the nose temperature, the critical time was about 4 s. According to the TTP curve, from Fig.3 we can find that the temperature of quenching sensitive interval is 270~90 °C. In this range, supersatu-

rated solid solutions of alloy is most easily decomposed, the quenching sensitivity of the specimens is much higher, and the rate of phase transition is faster than that at other temperatures.

2.3 DSC study of the isothermal phase transformation

The DSC curves of quenched alloy held at 330 °C for different time are shown in Fig.5. The scan from the specimens, which is quenched and naturally aged for 3 d, clearly shows 4 peaks corresponding to the 4 types of precipitates (see Fig.5). The peak evolution is consistent with other studies^[24]. In the fast quenching, the first exothermic peak (~85 °C) is most likely associated with the formation of solid solution clusters and the precipitation of GPI zones, but the peak is not significant because some pre-existing GP zones have been formed in the process of natural aging. The second peak corresponds to a higher temperature (heated to 176 °C), which indicates that the η' phase is formed at this time. The third peak (~224 °C) is related to the precipitation of the η phase. Besides the η phase, the fourth peak is also likely associated with the formation of S or T phase. Therefore, it can be concluded that the precipitation sequence of experimental alloy is supersaturated solid solu-

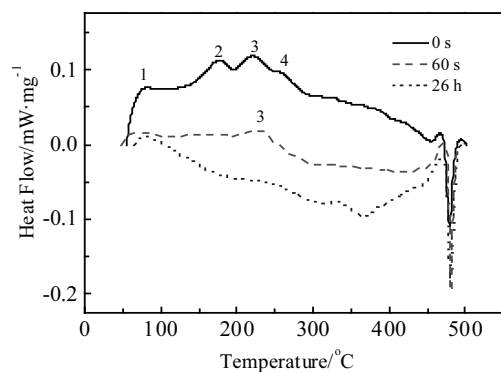


Fig.5 DSC curves of as-quenched Al-9.0Zn-2.5Mg-1.5Cu-0.15 Zr-0.2Sc alloy for different isothermal time

tion-GP zones- η' precipitation- η precipitation-S or T precipitation. When isothermally held for 60 s, only one exothermic peak appeared on the DSC curve. It means that only η phase is formed. When the isothermal holding time was prolonged to 26 h at 330 °C, there was no exothermic peak. The results show that the supersaturated solid solution is decomposed and the second phase is precipitated completely in the isothermal treatment.

2.4 Kinetics study of the isothermal phase transformation

The precipitation sequence of Al-Zn-Mg-Cu-Zr-Sc alloy was mentioned previously. The density of GP zones and the precipitation of η' phase determine the performance of experimental alloy. Large numbers of studies have shown that high concentrations of solutes and vacancies lead to high-density of GP zones. Furthermore, isothermal holding for a long time in the salt bath reduces the vacancy concentration, because vacancy diffusion is partly responsible for the quenching sensitivity of Al-Zn-Mg-Cu alloy. Therefore, with the prolongation of the holding time, the GP zone and the η' precipitation are more difficult to be found.

The Johnson-Mehl-Avrami equation (Eq.(1))^[25] can represent the kinetics of the isothermal phase transition:

$$f = 1 - \exp(-kt^n) \quad (1)$$

$$\ln[-\ln(1-f)] = \ln k + n \ln t$$

where, f represents the volume fraction of the new precipitated phase at time t , k represents the Avrami constant, which is affected by phase change temperature and grain size, and n

is the Avrami exponent, which is related to the nucleation position and type of phase transition.

The Avrami parameter k values fitted by Origin 8.5 are shown in Fig.6. It has been confirmed that the rate of phase transition is closely associated with the value of k ^[26]. The larger the k value, the faster the nucleation growth and transformation. Therefore, it is evident that the k value reaches a maximum at 330 °C, and accordingly, the phase transition rate is maximum at this temperature.

For aluminum alloys, undercooling and atomic diffusion rate are two main factors that affect the quenching sensitivity^[26]. At high temperature, the samples have small nucleation rate because of low supersaturation and small driving force of precipitation. The second phase is mainly precipitated by inhomogeneous nucleation. Thus, the nucleation rate and precipitation rate are both slow though the diffusion rate is fast. At low temperature, although the supersaturation and driving force are very large, due to the low temperature, the diffusion rate and second phase growth rate are slow. So the precipitation rate is still very small. Only at medium temperature can there be sufficient driving force and temperature, and the precipitation rate is the fastest.

2.5 XRD study of the isothermal phase transformation

The experimental alloy was analyzed by XRD after isothermal holding at 330 °C for 0 s, 60 s, and 26 h. The main phases after peak-aging treatment are α -Al and MgZn₂ phase (see Fig.7). The samples of heat preservation for 0 s (i.e.,

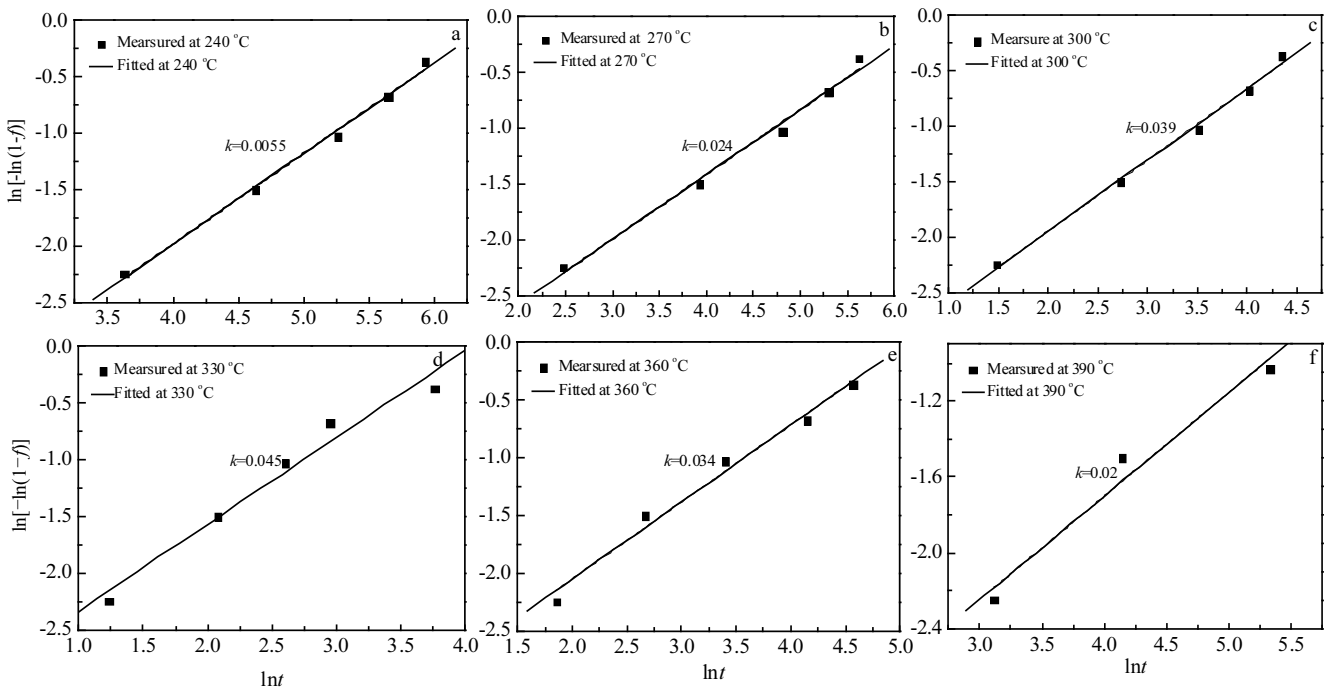


Fig.6 k values obtained by Johnson-Mehl-Avrami equation fitted at different temperatures: (a) $k=0.0055$, (b) $k=0.024$, (c) $k=0.039$, (d) $k=0.045$, (e) $k=0.034$, and (f) $k=0.02$

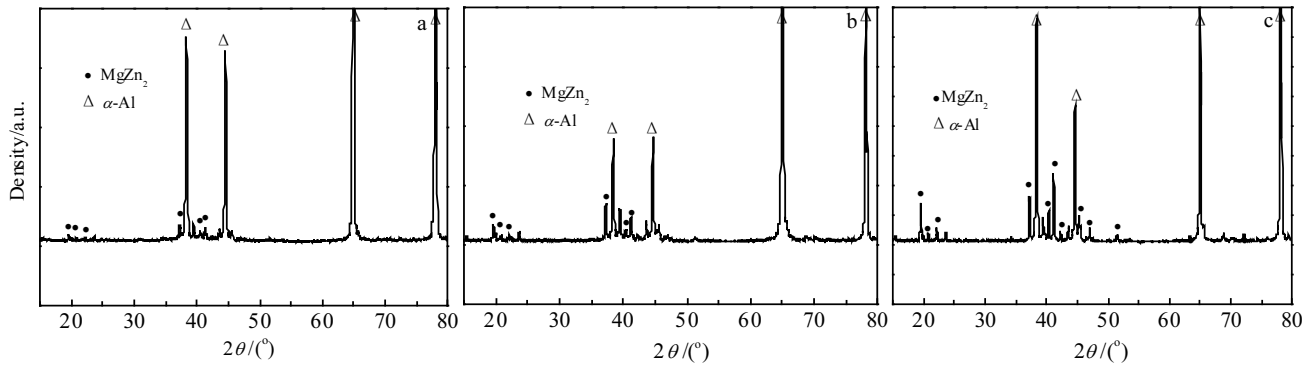


Fig.7 XRD patterns of peak aged Al-9.0Zn-2.5Mg-1.5Cu-0.15Zr-0.2Sc alloy for different isothermal time at 330 °C: (a) 0 s, (b) 60 s, and (c) 26 h

direct water quenching) contain a small amount of $MgZn_2$ phase in the matrix of α -Al (see Fig. 7a). With the increase of the isothermal time, the peak strength of $MgZn_2$ phase precipitation increased obviously (Fig. 7b). This indicates that more $MgZn_2$ is released. For the samples treated for 26 h, not only the highest peak corresponding to $MgZn_2$ phase appears in the spectrum (Fig. 7c), but also some new peaks appear, which are identified as $MgZn_2$ phase.

2.6 TEM study of the isothermal phase transformation

Fig. 8 shows the TEM images of experimental alloy after holding at 330 °C for different time and artificial aging. From Fig. 8a, high density η ' precipitates are uniformly distributed in the aluminum matrix. These particles can en-

hance the effect of reinforcement. With the extension of the holding time, the particles will be coarsened, as shown in Fig. 8b, 8c, 8e and 8f. When isothermal holding time was extended to 5 s, some stick-shaped equilibrium-state η particles appeared, as shown in Fig. 8b. When the time extended to 20 s, there were some coarse η precipitates with a length of 300 nm surrounded by precipitate free zone (PFZ), as shown in Fig. 8c. From Fig. 8e and 8f, when prolonging the holding time to 100 and 1500 s, a large amount of equilibrium-state η particles appeared in the grains, the size of which is obviously larger than that treated for 20 s. There are many $Al_3(Sc, Zr)$ dispersions in the grain (Fig. 8d). $Al_3(Sc, Zr)$ particles provide a favorable position for η

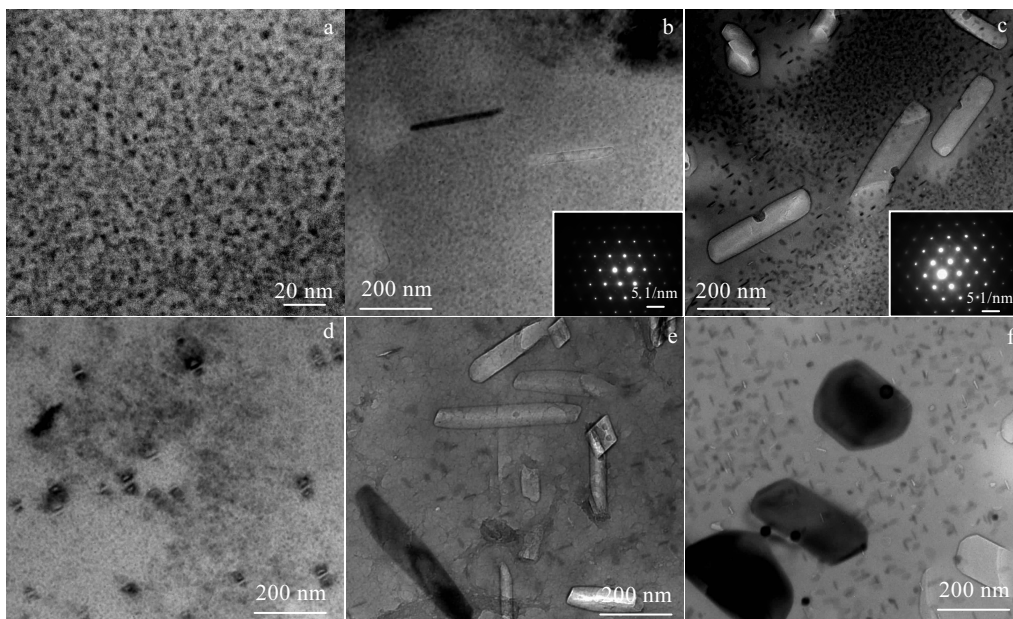


Fig.8 Morphologies of precipitates in matrix of peak-aged alloy after holding for different time at 330 °C (η is precipitation phase during holding treatment): (a) 0 s, (b) 5 s, (c, d) 20 s, (e) 100 s, and (f) 1500 s

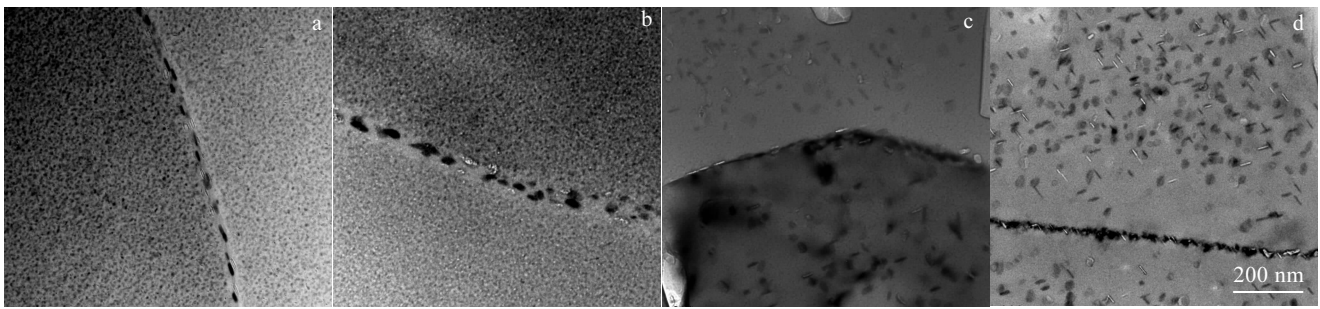


Fig. 9 Morphologies of precipitates at grain boundaries of peak-aged alloy after holding different time at 330 °C: (a) 5 s, (b) 20 s, (c) 100 s, and (d) 1500 s

phase nucleating and promote the precipitation and growth of η particles. As seen in Fig. 8c and 8f, the more heterogeneous the nucleation sites, the greater the number of coarse equilibrium phases, which accelerates the depletion of the solute atoms in the matrix. Consequently, there is precipitate free zone (PFZ) nearby these coarse phases.

Fig. 9 shows the morphologies of precipitates at grain boundaries of specimens after isothermal holding for different time at 330 °C and then artificial ageing at 120 °C for 24 h. From Fig. 9a, the equilibrium-state η particles at grain boundaries are discontinuous in the specimen after holding for 5 s, and at this stage, the PFZ is narrow. When the holding time is 20 s, the size of grain boundary precipitates is further increased, and particles are also discontinuous. The PFZ is wider than that held for 5 s (Fig. 9b). With prolonging the isothermal holding time to 100 s or 1500 s, the equilibrium-state η particles are distributed continuously on the grain boundaries. However, the PFZ becomes wider. But the width of PFZ in Fig. 9c and Fig. 9d is almost the same, which indicates that the solid solution reaches the steady state after being isothermally held at 330 °C for 100 s.

Al-Zn-Mg-Cu-Zr-Sc alloy is an age-hardenable alloy. In order to achieve the strengthening effect, it is necessary to control the decomposition of supersaturated solid solution to acquire hardening precipitates that are fine and uniformly distributed in the matrix. But inadequate quenching often leads to heterogeneous precipitation, namely more loss of solutes, which leads to the precipitation of coarse equilibrium phase, and smaller subsequent aging hardening effect can be obtained. It is the major reason for the quenching sensitivity^[27]. Prolonging the isothermal holding time will promote the decomposition of supersaturated solid solution, and the number of coarse equilibrium particles increases. Therefore, due to the less amounts of solutes, less volume of hardening precipitation is produced in subsequent aging processes, which results in the loss of hardenability. It can be observed that PFZ is presented around the quench-induced precipitates and the grain boundary, and the

width of the PFZ is broadened with the extension of the holding time. Thus, it seems that the PFZ is mostly related to the loss of solute caused by the quench-induced precipitation.

Furthermore, the large η particles preferentially nucleate on incoherent $\text{Al}_3(\text{Sc}, \text{Zr})$ dispersoids and high angle grain boundaries. The influence of Sc and Zr on quenching sensitivity is mainly classified into two aspects. For one thing, as complete recrystallization occurs in this alloy, the coherent $\text{Al}_3(\text{Sc}, \text{Zr})$ dispersoids lose their coherency with the matrix, thus becoming the core of heterogeneous nucleation and improving the quenching sensitivity of the Al-Zn-Mg-Cu alloys, which has an adverse influence on the performance of the alloy. For the other, according to previous work^[13], adding Sc and Zr can inhibit recrystallization and reduce the number of grain boundaries, which leads to low quenching sensitivity.

3 Conclusions

1) The TTP and TTT curves, which are obtained from the experimental results, are characterized by a C-shape with a nose temperature of 330 °C and the quenching sensitivity temperature range is 270~390 °C. The optimum quenching condition for the alloy is rapid cooling in the critical temperature range of 270~390 °C and slower cooling in the high or low temperature range, which can lead to high mechanical properties and low residual stress.

2) The Avrami parameter k values reach a maximum at 330 °C, indicating that the rate of phase transition is the fastest at this time.

3) $\text{Al}_3(\text{Sc}, \text{Zr})$ dispersoids are more effective sites for η phase that is nucleated heterogeneously and precipitated from the supersaturated solid solution of Al-9.0Zn-2.5Mg-1.5Cu-0.15Zr-0.2Sc alloy within the critical temperature range.

4) The influence of rare-earth element Sc and Zr on quenching sensitivity of Al-Zn-Mg-Cu alloy is reflected in the level of inhibiting recrystallization and the distribution of $\text{Al}_3(\text{Sc}, \text{Zr})$ particles.

References

- 1 Williams J C, Starke E A. *Acta Mater*[J], 2003, 51(19): 775
- 2 Huda Z, Edi P. *Materials & Design*[J], 2013, 46(4): 552
- 3 Lin Lianghua, Liu Zhiyi, Bai Song et al. *Materials & Design*[J], 2015, 86(1): 679
- 4 Liu S D, Chen B, Li C B et al. *Corrosion Science*[J], 2015, 91(2): 203
- 5 Tiryakiolu M, Robinson J S, Eason P D. *Materials Science & Engineering A*[J], 2014, 618(11): 22
- 6 Zheng Yulin, Li Chengbo, Liu Shengdan et al. *Transactions of Nonferrous Metals Society of China*[J], 2014, 24(7): 2275
- 7 Zhang Yong, Milkereit B, Kessler O et al. *Journal of Alloys & Compounds*[J], 2014, 584(3): 581
- 8 Starink M J, Mikereit B, Zhang Yong et al. *Materials & Design*[J], 2015, 88(12): 958
- 9 Nie Baohua, Liu Peiying, Zhou Tietao. *Materials Science & Engineering A*[J], 2016, 667(6): 106
- 10 Lin lianghua, Wan Li, Zhang Yunya et al. *Materials Science and Engineering A*[J], 2017, 682(1): 640
- 11 Dorin Thomas, Ramajayam Mahendra, Lamb Justin et al. *Materials Science and Engineering A*[J], 2017, 707(11): 58
- 12 Deng Ying, Xu Guofu, Yin Zhimin et al. *Journal of Alloys & Compounds*[J], 2013, 580(12): 412
- 13 Shi Yunjia, Pan Qinglin, Li Mengjia et al. *Materials Science & Engineering A*[J], 2015, 621(1): 173
- 14 Sun Fangfang, Liu Guiru, Li Qunying et al. *Journal of Materials Science & Technology*[J], 2017, 33(9): 1015
- 15 Røyset J, Ryum N. *International Materials Reviews*[J], 2005, 50(1): 19
- 16 Li J H, Oberdorfer B, Wurster S et al. *Journal of Materials Science*[J], 2014, 49(17): 5961
- 17 Li Jiehua, Wiessner M, Albu M et al. *Materials Characterization*[J], 2015, 102(4): 62
- 18 Morrison C B, Seidman D N, Dunand D C. *Acta Materialia*[J], 2012, 60(8): 3643
- 19 Duan Y L, Xu G F, Peng X Y et al. *Materials Science & Engineering A*[J], 2015, 648(11): 80
- 20 Lee S L, Wu C T, Chen Y D. *Journal of Materials Engineering & Performance*[J], 2015, 24(3): 1165
- 21 Vlach M, Stulikova I, Smola B et al. *Materials Characterization*[J], 2013, 86(8): 59
- 22 Starink M J, Milkereit B, Zhang Yong et al. *Materials & Design*[J], 2015, 88(12): 958
- 23 Elgallad E M, Zhang Zhan, Chen X G. *Materials Science & Engineering A*[J], 2015, 625(2): 213
- 24 Li Shenlan, Huang Zhiqi, Chen Weiping et al. *Transactions of Nonferrous Metals Society of China*[J], 2013, 23(1): 46
- 25 Wang Huimin, Yi Youping, Huang Shiquan. *Journal of Alloys & Compounds*[J], 2017, 690(1): 446
- 26 Xiong Baiqing, Li Xiwu, Zhang Yongan et al. *Chinese Journal of Nonferrous Metals*[J], 2011, 21(10): 2631 (in Chinese)
- 27 Conserva M, Fiorini P. *Metallurgical and Materials Transactions B*[J], 1973, 4(3): 857

Al-9.0Zn-2.5Mg-1.5Cu-0.15Zr-0.2Sc 合金淬火性能及 TTT 和 TTP 曲线

戴晓元, 熊超宇, 李 妮, 罗奕兵

(长沙理工大学 工程车辆轻量化与可靠性技术重点实验室, 湖南 长沙 410114)

摘要: 通过分级淬火处理得到 Al-9.0Zn-2.5Mg-1.5Cu-0.15Zr-0.2Sc 铝合金的时间-温度-转变 (TTT) 曲线和时间-温度-性能 (TTP) 曲线, 采用透射电子显微镜 (TEM)、差示扫描量热仪 (DSC) 和 X 射线衍射 (XRD) 对合金进行了相变分析。结果表明: 在一定的温度下延长保温时间会导致试样的电导率增加, 硬度降低。显微组织观察表明, 随着保温时间的增加, 许多大型杆状平衡相 η (MgZn_2) 会在基体中析出并快速生长, 导致淬火过程中溶质损失, 削弱了随后的时效强化效果。 η 粒子沉淀析出的主要原因是溶质原子的快速扩散和强大的相变驱动力。淬火敏感温度范围为 270~390 °C。因此, 在淬火敏感温度范围内, 需适当提高冷却速度以获得较高的力学性能。其他温度范围内应考虑适当降低冷却速度以控制残余应力。

关键词: Al-9.0Zn-2.5Mg-1.5Cu-0.15Zr-0.2Sc 合金; TTT 曲线; TTP 曲线; 无沉淀析出区 (PFZ)

作者简介: 戴晓元, 女, 1970 年生, 副教授, 博士, 长沙理工大学汽车与机械工程学院, 湖南 长沙 410114, E-mail: 542047849@qq.com